Solubilization of Phenol in an Intercalated Surfactant Bilayer

N. V. Venkataraman and S. Vasudevan*

Department of Inorganic and Physical Chemistry,Indian Institute of Science, Bangalore 560012, India

Received: October 3, 2002; In Final Form: February 24, 2003

Solubilization of phenol molecules in an intercalated surfactant bilayer, formed within the galleries of an inorganic layered solid, $CdPS_3$, is reported. The bilayer, formed by grafting of cetyl trimethylammonium (CTA) ions to the internal surface of $CdPS_3$, functionlizes the surface, converting it from a hydrophilic to a hydrophobic surface. The CTA ions being devoid of functional groups, the interaction between the guest phenol molecules and the methylene chains of the bilayer are dispersive in nature. It is shown that there are two phases of the phenol-solubilized intercalated bilayer, distinguishable by their interlayer lattice spacing and corresponding to solubilized phenol to intercalated CTA ion concentration ratios less than 0.5 and greater. The presence of the guest phenol, which is rotationally mobile, induces conformational disorder in the methylene chains of the intercalated bilayer. The nature and extent of conformational disorder have been studied using infrared and Raman vibrational spectroscopy and ^{13}C CP-MAS NMR spectroscopy. Conformational disorder in the two phases of the phenol-solubilized bilayer is different, and the observed differences in the interlayer lattice spacings have been related to differences in the nature of conformational disorder.

Introduction

Inorganic layered solids functionalized by intercalation of long-chain surfactants find several applications, including removal of organic pollutants in water treatment[1−4] and as precursors in the synthesis of polymer intercalated nanocomposites.[5−7] Functionalization converts the essentially hydrophilic internal surface of the inorganic solid to one that is hydrophobic, capable of solubilizing nonpolar as well as poorly water-soluble guest molecules.[8] In such situations, the intercalated surfactant may be considered as the host or alternatively as a two-dimensional solvent.[9] Most applications of these organic−inorganic hybrids have, indeed, been based on the ability of the intercalated surfactant to solubilize neutral organic molecules within the interlayer space of an inorganic layered solid.[8] The process, termed as "adsolubilization",[10] has been utilized to confine a variety of "guest" species from simple organic solvents such as toluene[11] to photoactive aromatic hydrocarbons[12,13] and polymers[5−7] within the surfactant intercalated layered "hosts".

The utility of surfactant intercalated clays, the so-called "organo-clays",[14,15] for the removal of phenolic pollutants in water treatment has been demonstrated and the adsolubilization of phenol and its derivatives by a variety of surfactant intercalated clays reported.[1,2] Most studies have focused exclusively on the measurement of adsorption isotherms[1−4] and the efficiency of different types of surfactants intercalated in clays for the removal of these pollutants.[1,2,9] Structural characterization of these compounds with the adsolubilized guest has largely been restricted to powder X-ray diffraction studies.[1,11] The effect of adsolubilization of small organic guest molecules on the conformation and organization of alkyl chains of intercalated surfactant as well as the nature of interaction between guest and the intercalated surfactant host, however, remains a less widely explored aspect. Characterizing conformational changes on adsolubilization as well as understanding the host−guest interactions is of fundamental interest and a prerequisite not only for a better understanding of the adsolubilization process for removal of pollutants but also for a molecular level understanding of the mechanism of retention in reversed phase chromatography.[16]

The layered host chosen in the present study is Cadmium thiophosphate.[17,18] Its host−guest chemistry is representative of many layered inorganic solids, e.g., the mica-type silicates, but at the same time has the advantage that single crystals can be easily obtained whose integrity is preserved even on intercalation. Additionally, it offers a convenient window for spectral studies of the intercalated guest. Cadmium thiophosphate is formed by the stacking of $CdPS_3$ sheets, built from CdS_6 and P_2S_6 polyherdra, with a van der Waals gap of 3.2 Å.[18] It undergoes an interesting ion-exchange intercalation reaction in which cationic species are introduced into the van der Waals gap with an equivalent loss of cadmium ions from the layer.[19−21] The interlamellar cations may be further ion-exchanged with either inorganic or organic cations. We have previously shown that long-chain cationic cetyl trimethylammonium (CTA) ions, $[C_{16}H_{33}N^+(CH_3)_3]$, can be introduced into the galleries of cadmium thiophosphate, $CdPS_3$, by ion-exchanging the interlamellar hydrated K^+ ions in $Cd_{0.83}PS_3K_{0.34}(H_2O)$ with CTA ions to give $Cd_{0.83}PS_3(CTA)_{0.34}$.[22] Intercalation occurs with a lattice dilation of 26.5 Å as compared to pristine $CdPS_3$. The intercalated surfactants form a bilayer with the cationic headgroup anchored at the negatively charged cadmium deficient $Cd_{0.83}PS_3$ sheets. Spectroscopic studies had established that a majority of the methylene units of the bilayer adopt the trans configuration and that the methylene chains are tilted at an angle of 55° with respect to the interlayer normal.[22] This tilt angle is consistent with the value calculated from the lattice expansion and the length of the all-trans CTA ion (∼22 Å).

Here we report a detailed study of the adsolubilization of phenol by the intercalated surfactant bilayer in $Cd_{0.83}PS_3(CTA)_{0.34}$. In addition to characterizing the adsolubilized phase,

* To whom correspondence should be addressed. E-mail: svipc@ipc.iisc.ernet.in.

10.1021/jp027124d CCC: $25.00
Published on Web 05/03/2003

the present study also focuses on the nature of interaction of the adsolubilized phenol with the intercalated surfactant and the effect of adsolubilization on the conformation and organization of the methylene chains of the intercalated surfactant bilayer, using spectroscopic techniques. Our results provide a molecular level picture of the adsolubilization process. Additionally, because the intercalated surfactant bilayer bears a striking structural resemblance to lipid bilayers, a major component of biomembranes, these results are relevant to understanding partitioning of solutes in lipid bilayers, a process crucial for molecular transport in and out of cells.

Experimental Section

Cadmium thiophosphate, $CdPS_3$, was prepared from the elements following the procedure reported in the literature.[23] Cadmium metal powder, phosphorus, and sulfur in stoichiometric amounts were sealed in quartz ampules at 10^{-6} Torr and heated at 650 °C for two weeks. Single crystals of $CdPS_3$ were grown by chemical vapor transport using excess sulfur as a transporting agent. Cetyl trimethylammonium bromide (CTAB) (Loba Chem) was recrystallized from acetone/methanol.

Intercalation of CTA ions was effected by a two-step ion-exchange process.[22] In the first step, hydrated potassium ions are ion-exchange intercalated by treating $CdPS_3$ with a 4 M aqueous solution of potassium chloride in the presence of 0.1 M EDTA and 1 M $K_2CO_3/KHCO_3$ as buffer, to give $Cd_{0.83}PS_3K_{0.34}(H_2O)$

$$CdPS_3 + 2xK^+(aq) \xrightarrow{\text{EDTA}} Cd_{1-x}PS_3K_{2x}(H_2O)_y + Cd_{(aq)}^{2+} \quad (x = 0.17)$$

This compound has a lattice spacing of 9.4 Å, corresponding to a lattice expansion of 2.8 Å as compared to pristine host $CdPS_3$.[19,21] The interlamellar potassium ions in $Cd_{0.83}PS_3K_{0.34}(H_2O)$ were further ion-exchanged with cetyl trimethylammonium (CTA) ions, by refluxing in an aqueous solution of 0.05M CTAB at 50 °C for 6 h, to give $Cd_{0.83}PS_3(CTA)_{0.34}$

$$Cd_{1-x}PS_3K_{2x}(H_2O)_y + 2xCTA^+(aq) \rightarrow Cd_{1-x}PS_3(CTA)_{2x} + 2xK^+(aq) \quad (x = 0.17)$$

Completion of ion-exchange was ascertained from the disappearance of the 00*l* reflection of $Cd_{0.83}PS_3K_{0.34}(H_2O)$ in the X-ray diffraction pattern and the appearance of a new series of 00*l* reflections with a lattice spacing of 33.0 Å corresponding to the formation of the intercalated surfactant bilayer phase, $Cd_{0.83}PS_3(CTA)_{0.34}$. Cadmium ion stoichiometry was established by atomic absorption spectroscopy (Perkin-Elmer 4381) and that of the intercalated CTA ion by CHN analysis (Cd, 29.5%; C, 23.95%; N, 1.53%; H, 4.51%).

Adsorption of phenol by the intercalated surfactant bilayer phase, $Cd_{0.83}PS_3(CTA)_{0.34}$, was measured at 298 K. Adsorption isotherms were obtained by equilibrating 100 mg quantities of $Cd_{0.83}PS_3(CTA)_{0.34}$ with 10 mL aliquots of hexane containing varying amounts of phenol, 0.1−1 mM for a period of 24 h. The concentration of the adsolubilized-phenol was obtained as a difference in concentration of phenol in solution before and after equilibration, by monitoring the intensity of the phenol $\pi \rightarrow \pi^*$ transition at 270 nm.

Powder X-ray diffraction patterns were recorded on a Shimadzu-XD-D1 diffractometer using Cu Kα radiation. FT-Raman spectra were recorded on Bruker IFS FT-Raman spectrometer, using a Nd:YAG (wavelength 1.064μm) laser as exciting radiation. All spectra were recorded at 4 cm^{-1} resolution with an unpolarized beam. Laser power was kept at 100 mw and typically ∼400 spectra were co-added to improve the signal-to-noise. ^{13}C CP-MAS NMR were recorded on a Bruker DSX-300 solid-state spectrometer at a Larmor frequency of 75.46 MHz with a contact time of 1 ms. The spectra were externally referenced to tetramethylsilane (TMS). Infrared spectra were recorded at 4 cm^{-1} resolution in the spectral range 400−4000 cm^{-1} on a Bruker IFS55 spectrometer. Samples were mounted on a hollow copper block and cooled using a CTI−Cryogenics closed cycle cryostat. Sample temperature could be varied from 300 to 50 K. Infrared spectrum for different orientations of the electric field vector (**E**) of the incident IR beam and the interlamellar normal (**C***) were recorded by an arrangement described in ref 24 and 25. In this arrangement the crystals are held in the sample block of the cryostat in such a way that the **C*** axis of the platelet-like crystal is at an angle of 45° with respect the propagation vector of the incident IR beam. From a measurement of the IR spectrum for two different angles of polarization of the electric field vector, **E**, the spectra for **E**⊥**C*** and **E**∥**C*** could be recovered and subsequently, the spectrum for any orientation, ϕ, of **E** with respect to **C*** could be calculated.

Results

Adsorption of Phenol. Figure 1a shows the adsorption isotherm measured at 298 K for the adsorption of phenol from hexane solution by the intercalated surfactant bilayer, $Cd_{0.83}PS_3(CTA)_{0.34}$. The amount of phenol adsorbed by the intercalated surfactant, expressed as the molar ratio of adsorbed phenol to CTA ions in the intercalated bilayer phase (henceforth referred to as the phenol/CTA ratio), is plotted as a function of the concentration of phenol in the hexane solution. The adsorption isotherm, Figure 1a, does not resemble a Langmuir isotherm and in fact shows two regions. It may be seen from Figure 1a that the slope of the adsorption isotherm changes above a phenol/CTA ratio of ∼0.5. Below this concentration, the adsorption rises steeply with increasing concentrations of phenol in solution, whereas above a phenol/CTA ratio of ∼0.5 the rise is more gradual. The adsorption isotherm clearly indicates that there are two different regimes ("phases") of the intercalated bilayer depending on the concentration of adsolubilized-phenol. An alternate representation of the adsorption is by considering the adsolubilization process as the partitioning of phenol (solute) between hexane and the intercalated surfactant bilayer phase.

Partition coefficients of solutes in micellar phases of surfactants have been widely reported.[26] The reported values of the partition coefficient, **K**, differ widely depending on the choice of units used for expressing concentrations as well as the definition of the partition coefficient.[26] These definitions are, however, not directly applicable to the partitioning of a solute between liquid and solid phase. We define the partition coefficient for the adsolubilization of phenol, based on molar ratios

$$\mathbf{K} = X_{solid}/X_{liquid}$$

where X_{solid} is the mole fraction of solute in the solid-phase calculated as X_{solid} = (number of moles of adsolubilized-phenol)/(number of moles of intercalated CTA ions) and X_{liquid} is the mole fraction of phenol in the hexane solution. The partition coefficient of phenol, so calculated, is plotted in Figure 1a as a function of the phenol concentration in solution. It is, however, more illustrative to plot the partition coefficient as a function of phenol/CTA ratio (Figure 1b). The partition coefficient has

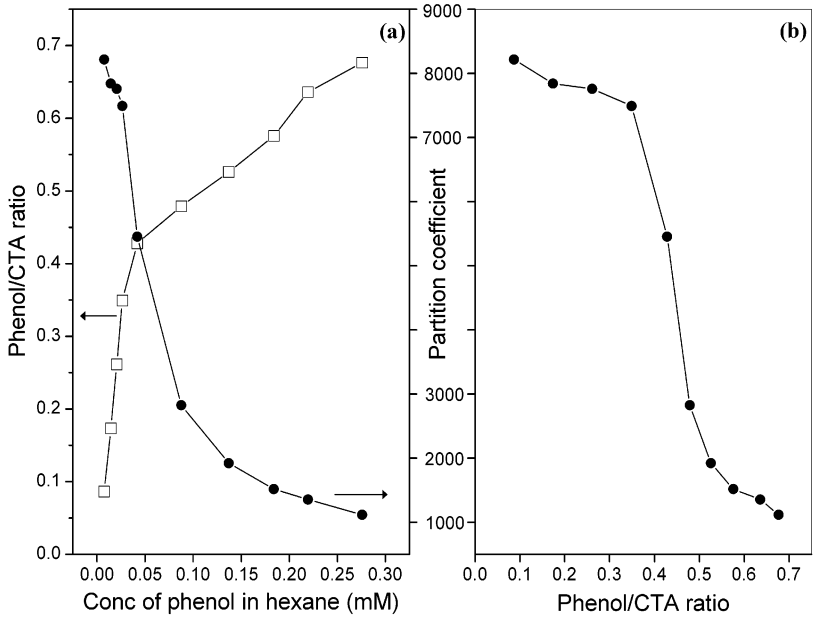

Figure 1. (a) Adsorption isotherm (open squares) for the adsolubilization of phenol by the intercalated surfactant bilayer $Cd_{0.83}PS_3(CTA)_{0.34}$ at 298 K. The molar ratio of adsolubilized phenol to intercalated CTA ion has been plotted as a function of the concentration of phenol in hexane solution. The corresponding changes in the partition coefficient (see text) are also plotted (closed circles). (b) Change in partition coefficient as a function of the phenol/CTA ratio.

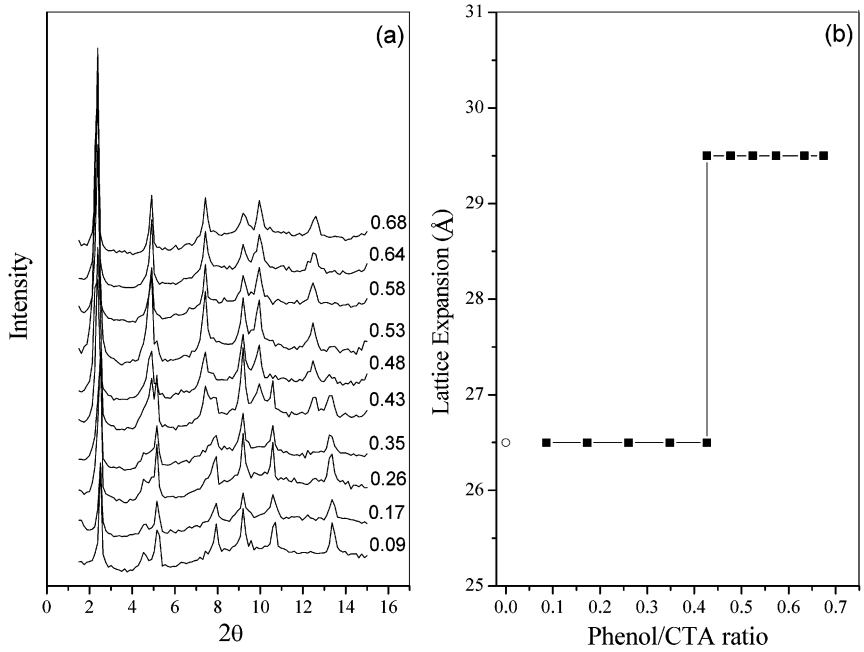

Figure 2. (a) Powder X-ray diffraction patterns of phenol-adsolubilized−intercalated-surfactant bilayer, $Cd_{0.83}PS_3(CTA)_{0.34}(phenol)_y$, phases for different phenol/CTA ratios (the ratios are indicated alongside). (b) Variation in the interlayer expansion of the phenol adsolubilized phases for different phenol/CTA ratios. The lattice expansions are with respect to the pristine host $CdPS_3$.

clearly two different values. For a concentration ratio of phenol to intercalated CTA (phenol/CTA) less than 0.5, the coefficient has a value of ∼8000 (this region corresponds to the steep increase in the adsorption isotherm) and above a ratio of 0.5 the partition coefficient has a much smaller value of ∼1000. To understand whether there are structural differences in the intercalated phases in these two regions, powder X-ray diffraction of the intercalates as a function of the concentration of adsolubilized-phenol was recorded.

X-ray Diffraction. Figure 2a shows the powder X-ray diffraction patterns of the phenol-adsolubilized−intercalated-surfactant bilayer phase, $[Cd_{0.83}PS_3(CTA)_{0.34}(phenol)_y]$, for different phenol/CTA ratios. Because of the layered nature of the intercalated compounds, the crystallites exhibit a pronounced preferred orientation, and consequently, only 00*l* reflections are seen in the XRD pattern. For phenol/CTA ratio below ∼0.5 the 00*l* reflections correspond to a unique interlayer spacing (33.0 Å) which is identical to that of the starting intercalated surfactant bilayer.[22] For phenol/CTA ratios above ∼0.5, the 00*l* reflections could be indexed to an interlayer spacing of 36.0 Å which corresponds to a lattice expansion of 3.0 Å with respect to the parent intercalated bilayer. At a phenol/CTA ratio of ∼0.5, both the reflections are seen. The expansion of the interlayer spacing of $Cd_{0.83}PS_3(CTA)_{0.34}(phenol)_y$ as a function of the phenol/CTA ratio is plotted in Figure 2b. The lattice expansions are with respect to the pristine host $CdPS_3$.

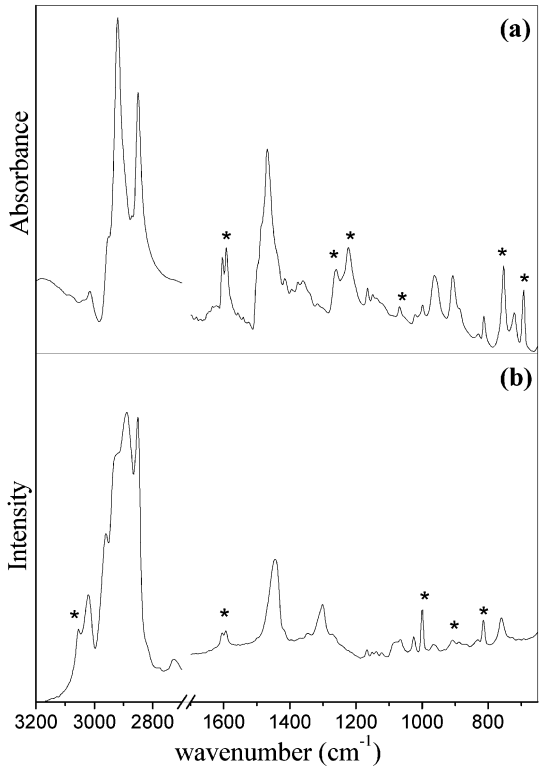

Figure 3. (a) Infrared and (b) Raman spectra of the phenol-adsolubilized−intercalated-surfactant bilayer, $Cd_{0.83}PS_3(CTA)_{0.34}(phenol)_{0.23}$, [phenol/CTA = 0.68]. The bands due to adsolubilized phenol are indicated.

It may be seen that up to a phenol/CTA concentration of 0.5 the intercalated bilayer can accommodate the guest, phenol, with no change in the thickness of the bilayer. Because the surfactant molecules are grafted onto the rigid inorganic $Cd_{0.83}PS_3$ sheets, lateral expansion is ruled out. Above a phenol/CTA concentration of 0.5, the bilayer thickness has to expand if further phenol molecules have to be accommodated. The XRD results confirm the results of the adsorption measurements that there are two distinct phases of $Cd_{0.83}PS_3(CTA)_{0.34}(phenol)_y$ corresponding to phenol/CTA ratios below ~0.5, characterized by a lattice spacing of 33.0 Å and above ~0.5, where the lattice spacing is 36.0 Å. These two phases may thus be distinguished by their interlayer spacing.

Vibrational Spectroscopy. Typical infrared and Raman spectra of the phenol-adsolubilized-intercalated-surfactant bilayer $[Cd_{0.83}PS_3(CTA)_{0.34}(phenol)_y]$ are shown in Figure 3, parts a and b. The spectra are for a sample corresponding to a phenol/CTA ratio of 0.68. Both the IR and Raman spectra show bands corresponding to the vibrational modes of the intercalated surfactant as well as those of the adsolubilized-phenol (marked by *). The positions of most features of the vibrational spectra do not show any significant change for different phenol/CTA ratios; the only change is in the relative intensities. (The observed band positions and their assignments are given as part of the Supporting Information.)

Bands Due To the Intercalated Surfactant.[22] The intense bands at 2852 and 2921 cm^{-1} in the infrared spectrum are assigned to the methylene symmetric and antisymmetric stretching modes of the alkyl chains of the intercalated CTA ion. The asymmetric and symmetric stretching modes of the terminal methyl groups are seen as weak features in the spectra at 2950 and 2871 cm^{-1}, respectively. The vibrational modes of the $N^+(CH_3)_3$ head group of the intercalated CTA ions are seen at 3016 and 1485 cm^{-1}. The former is assigned to the asymmetric C−H stretching, whereas the later are assigned to the symmetric bending. The bands at 965 and 912 cm^{-1} in the infrared spectrum are due to $C-N^+$ stretching modes of the head group. The methylene scissoring and rocking modes are seen at 1467 and 721 cm^{-1}, respectively. These modes are known to be sensitive to the packing arrangement in alkyl chain assemblies.[27,28] In an orthorhombic or monoclinic arrangement, these modes are split because of lateral interchain interactions, whereas splitting of these modes is absent in triclinic packing where there is only one chain per unit cell as well as in alkane chain assemblies of low density where lateral interchain interactions are weak. In the intercalated bilayer as well as the phenol adsolubilized bilayer phases, these modes appear as single component.

Raman spectrum of the phenol-adsolubilized bilayer shows bands corresponding to the methylene antisymmetric and symmetric C−H stretching modes of the intercalated CTA ions at 2882 and 2850 cm^{-1} respectively. The band at 1445 cm^{-1} is assigned to the methylene scissoring mode and the band at 1299 cm^{-1} to the methylene twisting mode. The C−C skeletal stretching modes of the intercalated CTA ion are seen at 1066 and 1135 cm^{-1}. The $C-N^+$ stretching mode of the head group appears at 761 cm^{-1}. The position of the vibrational bands due to the intercalated surfactant in both IR and Raman show no significant change in the presence of adsolubilized-phenol.

Bands Due To Adsolubilized Phenol—nature of Host−Guest Interactions. Several vibrational modes of the adsolubilized phenol could be identified and assigned in the infrared and Raman spectra of the phenol-adsolubilized-bilayer phase. The assignments are based on those reported for pure phenol.[29] The IR and Raman spectrum in the region of 1650−650 cm^{-1} where most phenolic bands occur has been expanded in Figure 4, parts a and b. The corresponding IR and Raman spectrum of pure phenol is also shown. It may be seen that the peak positions of the adsolubilized-phenol vibrational bands are comparable to that of pure phenol. The bands at 1068 and 1022 cm^{-1} in the infrared spectrum are assigned to the in-plane C−H bending modes of the adsolubilized phenol. These values are comparable to those of pure phenol, 1067 and 1024 cm^{-1}. The out-of-plane C−H bending modes in the infrared spectrum of the adsolubilized-phenol are seen at 885, 829, and 754 cm^{-1}, as compared to 884, 825, and 752 cm^{-1}, respectively, for pure phenol. The phenolic O−H deformation mode, which occurs at 1167 cm^{-1} in pure phenol, is seen at 1165 cm^{-1} for the adsolubilized-phenol molecules. The positions of the phenolic bands show no change with concentration of adsolubilized-phenol.

Several vibrational modes of the adsolubilized phenol could be identified in the Raman spectrum of the phenol-adsolubilized-bilayer phase, and their positions are similar to that observed in the IR spectrum (Figure 4b). The phenolic C−H stretching mode appears as a weak band at 3056 cm^{-1}. The bands at 1604 and 1594 cm^{-1} are assigned to the C═C ring stretching modes and those at 1151 and 1025 cm^{-1} to the out-of-plane C−H bending modes. The in-plane C−H bending modes of the adsolubilized-phenol molecules appear at 967 and 910 cm^{-1}. The O−H deformation mode of the adsolubilized-phenol molecules is seen at 1166 cm^{-1}.

The fact that most of the phenolic vibrational modes appear at almost the same frequency as in pure phenol suggests the absence of any specific chemical interaction of the adsolubilized-phenol with the intercalated CTA ions. This is not surprising because the intercalated CTA chains are devoid of any functional group and consequently hydrogen bonding interactions involving

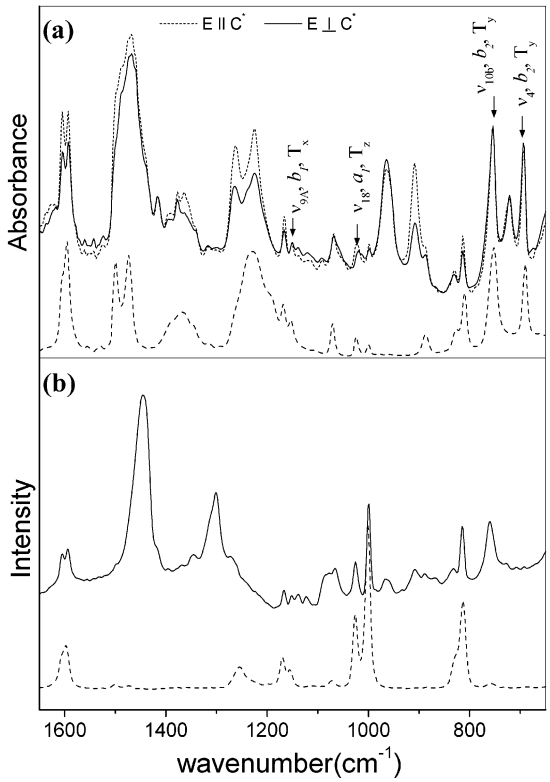

Figure 4. (a) Orientation-dependent infrared spectra of $Cd_{0.83}PS_3(CTA)_{0.34}(phenol)_{0.23}$, [phenol/CTA = 0.68] in the spectral region of the characteristic phenol vibrational modes. The spectra for two orientations, **E**⊥**C*** (solid line) and **E**||**C*** (dotted line), are shown; **C*** is the interlayer normal. For four of the phenol modes, the irreducible representations of the point group C_{2v} under which the modes transform are indicated. (b) The Raman spectrum of phenol-adsolubilized−intercalated-surfactant bilayer, $Cd_{0.83}PS_3(CTA)_{0.34}(phenol)_y$, [phenol/CTA = 0.68] in the 1650−650 cm^{-1} spectral region. In both the panels, the spectrum of pure phenol is shown in dashed lines.

the phenolic −OH groups are absent. The interactions between the adsolubilized-phenol and the intercalated CTA ion are, probably, purely dispersive in character.

Orientation Dependent Infrared Spectra. The orientation-dependent infrared spectra of crystals of $Cd_{0.83}PS_3(CTA)_{0.34}[phenol]_y$ were recorded to determine the orientation of the adsolubilized-phenol with respect to the bilayer normal. The infrared spectra of crystals of $Cd_{0.83}PS_3(CTA)_{0.34}[phenol]_y$ (phenol/CTA = 0.68) for two orientations, **E**||**C*** and **E**⊥**C**, in the region of the phenolic modes is shown in Figure 4a. Attention is focused on the phenolic modes at 1152 (ν_{9a}) and 1024 cm^{-1} (ν_{18}), the in-plane ═C−H bending modes, the 754 cm^{-1} (ν_{10b}) out-of-plane ═C−H bending mode, and 692 cm^{-1} (ν_4) ring deformation mode (these assignments and labeling are from refs 29 and 30). These infrared active modes belong to irreducible representations whose transformation properties lie along mutually orthogonal directions. The 1152 cm^{-1} in-plane C−H bending mode (ν_{9A}) transforms as the b_1 (T_x) of the C_{2v} point group, the 1024 cm^{-1} in-plane ═C−H bending mode (ν_{18}) as a_1 (T_z), and the 754 (ν_{10b}) and 692 cm^{-1} (ν_4) as b_2 (T_y). It may be seen that within the experimental limits the intensities of the phenolic bands are similar for the **E**||**C*** and **E**⊥**C** orientations. At lower concentration of the adsolubilized-phenol, too, the intensities of the phenolic modes show no orientational dependence in the infrared spectra.

The intensity of a vibrational mode is maximum when the transition dipole moment of the mode is oriented parallel to the electric field vector of the exciting radiation. For a vibrational mode, identical intensities for the two orientations **E**⊥**C*** and **E**||**C*** would arise if the transitions dipole moment associated with that mode is randomly oriented with respect to the **C*** axis or at an angle of 45°. The fact that the vibrational modes of the adsolubilized phenol, irrespective of the transformation properties of the mode, show no orientation dependence implies either (i) that the adsolubilized-phenol molecules are oriented randomly with respect to the interlamellar normal or (ii) one (or two) of the molecular axes are oriented at an angle of 45° with respect to **C*** and the remaining oriented randomly. The bands due to the intercalated methylene chains, for example the 912 cm^{-1} C−N^+ stretching mode of the head group, show an orientation dependence due to the tilt of the chain; however, as will be described in the following sections, the all-trans order of the methylene chains is destroyed on adsolubilization of phenol, and hence, the tilt angle of the methylene chains of the bilayer is not defined.

Effect of Adsolubilization of Phenol on Alkyl Chain Conformation. The influence of the adsolubilized phenol on the conformation of the methylene chains of the intercalated bilayer was probed by vibrational and ^{13}C CP-MAS NMR spectroscopy. Although ^{13}C NMR provides information on local conformation,[31,32] vibrational spectra, depending on the spectral region chosen, can provide information on both local as well as long-range conformation of a methylene chain.[33−37]

C−H Stretching Region (Infrared). The infrared spectrum in the C−H stretching region (3200−2800 cm^{-1}) of the phenol adsolubilized intercalated bilayer for different concentrations of solubilized phenol are shown in Figure 5a. The spectra show two strong bands corresponding to the symmetric and antisymmetric stretching modes of the methylene units of the intercalated CTA ion. It is well-known that the positions of these modes are sensitive to the chain conformation, shifting to higher frequencies in the presence of gauche disorder. For an all-trans conformation typical values for the methylene symmetric (ν_{sym}) and antisymmetric (ν_{asym}) stretching modes are in the ranges 2846−2848 and 2916−2918 cm^{-1}, respectively.[35] With increasing gauche disorder, they shift to higher wavenumbers, typically to 2854−2856 cm^{-1} for ν_{sym} and 2924−2928 cm^{-1} for ν_{asym}.[36] It may be seen from Figure 5a that the methylene antisymmetric and symmetric stretching modes shift progressively to higher frequencies as the concentration of the adsolubilized phenol increases. For the pure intercalated bilayer, the methylene symmetric and antisymmetric stretching modes appear at 2849 and 2918 cm^{-1}, whereas for the intercalated bilayer with phenol/CTA = 0.68, they appear at 2852 and 2921 cm^{-1}. These results indicate that the alkyl chains of the intercalated CTA ions become increasingly disordered (increasing concentration of gauche conformers) as the concentration of adsolubilized phenol in the bilayer phases increases.

C−H Stretching Region (Raman). The Raman spectra in the C−H stretching region of the phenol-adsolubilized−intercalated-bilayer for different phenol/CTA ratios are shown in Figure 5b. Attention is drawn to the intensity of the methylene antisymmetric and symmetric stretching modes appearing at ∼2880 and ∼2850 cm^{-1}, respectively. The intensities of the antisymmetric C−H stretching mode at 2880 cm^{-1} and the symmetric mode at 2850 cm^{-1} (I_{2880}/I_{2850}) is characteristic of conformational disorder as well as packing in alkyl chain assemblies.[37−39] This ratio has been widely used in biomembrane and phospholipid literature to characterize disorder in a bilayer.[37] In crystalline hydrocarbons, the ratio is near 2, and in hydrocarbon melts, it is near 0.7.[38] The Raman spectra of the phenol-

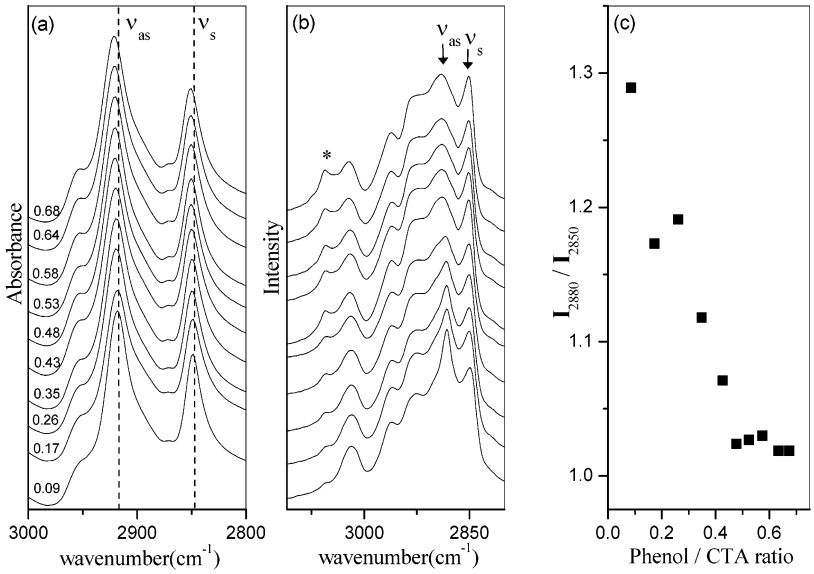

Figure 5. Infrared (a) and Raman (b) spectra of phenol-adsolubilized−intercalated-surfactant bilayer phases, $Cd_{0.83}PS_3(CTA)_{0.34}(phenol)_y$, for different phenol/CTA ratios as indicated in the figure. (c) The ratio of the intensities of the methylene antisymmetric to symmetric stretching modes in the Raman spectra, I_{2880}/I_{2850}, is plotted as a function of phenol/CTA ratio. (The band at 3056 cm^{-1}, indicated by an asterisk, is due to phenol).

adsolubilized-bilayer shows a large decrease in the intensity ratio I_{2880}/I_{2850} with increasing concentrations of phenol. In Figure 5c, this intensity ratio (I_{2880}/I_{2850}) has been plotted as a function of concentration of adsolubilized-phenol.

Figure 5c shows that disorder, as characterized by the I_{2880}/I_{2850} ratio, increases rapidly with increasing concentration of adsolubilized-phenol. The value of I_{2880}/I_{2850} decreases from 1.32 in the intercalated bilayer to 1.00 at a phenol/CTA ration of ~0.7. This decrease in the intensity ratio I_{2880}/I_{2850} could arise from conformational disorder as well as differences in the alkyl chain packing arrangement. The Raman spectra are in qualitative agreement with the results of the IR measurements that, too, indicated an increase in alkyl chain disorder with increasing concentration of adsolubilized-phenol. However, above a phenol/CTA ratio of 0.5, which corresponds to the formation of the second phase, there is no change in the Raman I_{2880}/I_{2850} ratio. This could imply either that there is no change in the conformation of the surfactant chain above a phenol/CTA ratio of 0.5 or that I_{2880}/I_{2850} is no longer sensitive to increasing conformational disorder. The latter is the more likely scenario because the typical range of the I_{2880}/I_{2850} ratios for a variety of alkyl chain systems is between 2.2 and 0.7.[38]

^{13}C CP-MAS NMR Spectroscopy. NMR spectroscopy has been widely used in the study of alkyl chain system like micelles, liquid crystals and surfactants.[40,41] In particular, ^{13}C NMR chemical shift differences have been used to characterize conformation of methylene chains.[31,32,42] It has been shown that the degree of shielding of a carbon atom in a methylene chain depends on the relative population of trans and gauche conformers, with the trans conformer giving rise to a downfield shift.[31] ^{13}C NMR is an ideal tool for probing the environment of the adsolubilized phenol and the methylene chains of the intercalated surfactant, since the resonances of the sp_2 carbons of the phenol would be well separated from the sp_3 carbons of the methylene chain of the CTA ions.

The^{13}C CP-MAS NMR spectrum of $Cd_{0.83}PS_3(CTA)_{0.34}$-$(phenol)_y$ [phenol/CTA = 0.68] is shown in Figure 6. The most surprising feature of the spectrum is the total absence of phenolic resonances. (The approximate expected positions of the phenol resonances are marked by arrows in Figure 6; the positions are for phenol in $CHCl_3$). This result is quite unexpected, because,

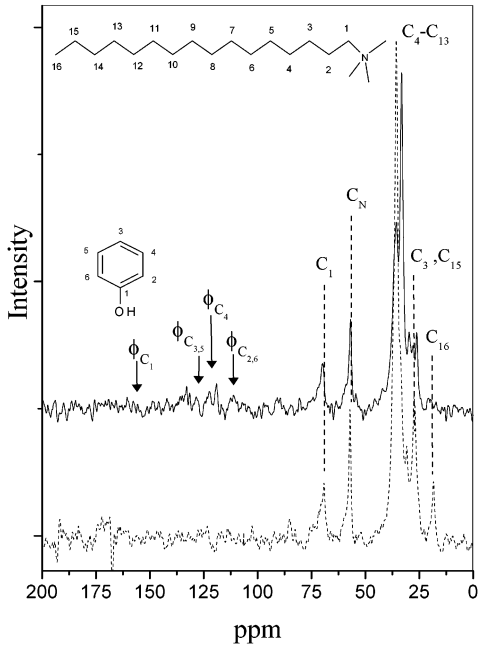

Figure 6. ^{13}C CP-MAS NMR spectrum of $Cd_{0.83}PS_3(CTA)_{0.34}(phenol)_y$ [phenol/CTA = 0.68] (solid line), along with the spectrum of the pure bilayer phase $Cd_{0.83}PS_3(CTA)_{0.34}$ (dotted line). The assignments of the methylene resonances and the labeling of the carbon atoms of the CTA ion are indicated. The expected positions and assignments of the phenolic resonances have been marked.

of all the phenol adsolubilized samples, this has the highest phenol/CTA ratio and for which in both the IR and Raman spectra the phenolic vibrational modes were quite intense (Figure 3). Also missing in the spectra of the phenol adsolubilized bilayer is the resonance of the terminal methyl (C_{16}) of the intercalated CTA ion, expected at 19.0 ppm. (The spectrum of the pure bilayer phase $Cd_{0.83}PS_3(CTA)_{0.34}$ is shown in dotted lines in Figure 6.) Another feature of the spectrum is the small, but significant, changes in the positions of the C_4 and C_{13} and C_3 and C_{15} resonances of the methylene chains in the presence of the adsolubilized-phenol. The positions of the C_1, C_N and C_2 resonances remain unchanged from that in the pure intercalated bilayer.

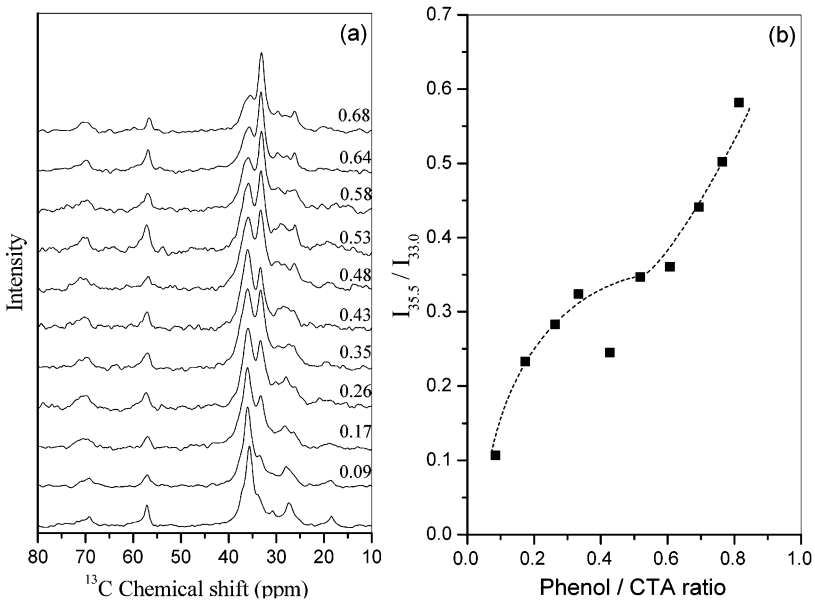

Figure 7. (a) ^{13}C CP-MAS NMR spectra of phenol-adsolubilized−intercalated-surfactant bilayer phases, $Cd_{0.83}PS_3(CTA)_{0.34}(phenol)_y$, for different phenol/CTA ratios.**(b)** The variation in the intensity ratio $I_{35.5}/I_{33.0}$ for different phenol/CTA concentration ratios.

The intensities of the resonances in a ^{13}C CP-MAS experiment depends, among other things, on the efficiency of the cross polarization (CP), the mechanism of which involves heteronuclear ^{13}C-^{1}H dipolar coupling.[43] In the presence of rapid motion, this dipolar coupling vanishes and the transfer of magnetization (^{1}H→^{13}C) by CP no longer exists. The absence of the resonances due to the phenol suggests the phenol molecules in the intercalated bilayer are rotationally mobile so that ^{13}C-^{1}H dipolar coupling are completely averaged (a more rigorous proof of this statement requires variable contact time CP MAS measurements, which are outside the scope of the present study). A similar argument may be used to explain the absence of the terminal C_{16} resonance of the intercalated surfactant chain. Rapid motion of the terminal methyl of the intercalated CTA ion of the adsolubilized bilayer is suggested by the ^{13}C NMR results.

Figure 7a shows the ^{13}C NMR spectra of the phenol adsolubilized bilayer for different phenol/CTA ratios in the region of methylene resonances. In none of the spectra were the phenol resonances observed, and consequently, the region where it is expected is not shown. The ^{13}C NMR spectra show a number of systematic trends. The positions of C_N, C_1, and C_2, irrespective of the phenol/CTA ratio, show no change from their positions in the pure intercalated surfactant bilayer. The resonance of the terminal C_{16} methyl group disappears with increasing concentration of phenol. At low concentration, e.g., the spectrum for the bilayer with the phenol/CTA = 0.09, it may still be seen, but at a slightly higher phenol/CTA ratio, 0.27, it is difficult to discern this resonance from the background. The resonance due to the C_3 and C_{15} carbons at 27.4 ppm shows an upfield shift with increasing phenol concentration reaching a value of 26.0 ppm for a phenol/CTA ratio of 0.68. The upfield shift is an indication of increase in gauche conformation at the C_3 and C_{15} positions in the CTA chain. The resonance of the C_4-C_{13} carbon atoms shows two resonance peaks, the relative intensities of which change with increasing phenol/CTA ratio. At low phenol/CTA ratio, the peak at 33.0 ppm is seen as a weak shoulder to peak at 35.5 ppm. At higher phenol/CTA ratios, the peak appearing at 33.0 ppm is more prominent with the peak at 35.5 ppm appearing as shoulder. The peak appearing at 35.5 ppm is assigned to a trans methylene sequence and the peak appearing upfield at 33.0 ppm to the presence of gauche conformers.[44] This difference in the resonance values is a consequence of the γ-gauche effect.[45]

The relative concentrations of the gauche to trans conformers in the interior, C_4-C_{13}, of the methylene chain of the intercalated bilayer may be estimated from the relative intensities of the peak at 35.5 and 33.0 ppm.[32] Relative intensities were estimated from a decomposition of the spectra as a sum of two Lorentzians. The intensity ratio ($I_{35.5}/I_{33.0}$) has been plotted in Figure 7b as a function of the phenol/CTA ratio. This intensity ratio corresponds to the ratio of the carbon atoms of the chain that feel the γ-gauche effect to those that do not. The relative concentration of gauche conformers increases with increasing concentration of adsolubilized phenol, in agreement with the IR and Raman results. The increase in the relative concentration is, however, not linear with the concentration of adsolubilized phenol. In fact it appears to level off at phenol/CTA ratio of ∼0.5 but then rises sharply above this concentration. It may be recalled that the adsorption/partition coefficient and the lattice spacings show different values above and below a phenol/CTA concentration of ∼ 0.5. Figure 7 indicates that this change is associated with a sharp increase in disorder in the interior C_4-C_{13} of the chains of the bilayer.

Long Range Conformation—Progression Bands in the Infrared Spectrum. In earlier publications,[44,46] we have shown that a significant fraction of the methylene chains in the intercalated bilayer $Cd_{0.83}PS_3(CTA)_{0.34}$ adopt a planar all-trans conformation at low temperature (50 K) with all fifteen methylene units of the chain in trans registry. Even at 300 K, although the population of all-trans chains is reduced, this fraction remains finite. This had been established from an analysis of the progression bands in the infrared spectrum of $Cd_{0.83}PS_3(CTA)_{0.34}$. These bands arise from a coupling of vibrational modes of methylene units in trans registry and manifest as a series of bands in the infrared spectrum.[47−49] The modes which give rise to the progression bands are the methylene rocking, twisting, wagging, and C−C stretching modes. The spacing of the progression bands is characteristic of the number of methylene units in trans registry.[50] The presence of a single gauche defect in a chain decouples the vibrational modes and such chains no longer contribute to the progression band

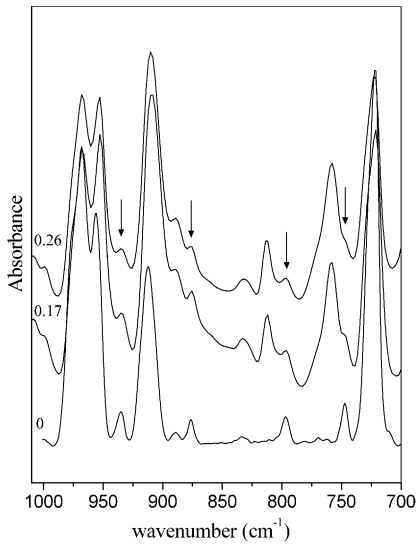

Figure 8. Infrared spectra in the region of methylene rocking-twisting progression bands for two different phenol/CTA ratios of the intercalated bilayer phases $Cd_{0.83}PS_3(CTA)_{0.34}(phenol)_y$ along with that of the pure bilayer $Cd_{0.83}PS_3(CTA)_{0.34}$. The spectra were recorded at 75 K.

intensity.[46] The intensity of the progression bands is, therefore, directly proportional to the concentration of planar all-trans methylene chains present in the intercalated bilayer. To study the effect of adsolubilization of phenol on the conformational order on the length scale of the methylene chains of the bilayer, the progression bands in the infrared spectra of $Cd_{0.83}PS_3(CTA)_{0.34}(phenol)_y$ were examined. For the adsolubilized bilayer, the progression bands were found to be extremely weak in intensity and further complicated by overlapping phenolic bands. Only the rocking-twisting modes of the methylene chain, which appear in the 1050−700 cm^{-1} region of the infrared spectra, could be seen and that too only at low temperature.

The progression bands in the infrared associated with the methylene rocking-twisting modes are shown in Figure 8, for two different phenol/CTA concentrations along with the spectra of the pure intercalated bilayer. The spectra were recorded at 75 K. The methylene rocking-twisting progression bands can be clearly seen for the pure bilayer phase at this temperature. For the phenol adsolubilized phases, however, these bands are much weaker in intensity and partly obscured by overlap with bands of the adsolubilized phenol (the progression bands are marked by arrows in Figure 8). The intensities of the progression bands are further reduced at higher phenol/CTA concentrations. The spectra shown in Figure 8 are for phenol/CTA concentration values of 0.17 and 0.26. For the next higher concentration corresponding to a phenol/CTA ratio of 0.35, these bands are so weak that it is difficult to distinguish the progression bands from the strong phenolic bands even at low temperatures (75 K). Figure 8, therefore, clearly indicates that the fraction of planar all-trans chains in the intercalated bilayer decreases dramatically in the presence of adsolubilized-phenol. It is clear, even from a conservative estimate, that planar all-trans alkyl chains are unlikely to be present in the intercalated bilayer when the phenol/CTA concentration ratio is 0.5 or greater.

Long Range Conformation—C−C Skeletal Stretching Mode (Raman). The progression bands in the infrared are intrinsically difficult to study because of their weak intensities. Additionally, for the phenol adsolubilized intercalated bilayer, there is interference from strong phenolic bands, which complicates analysis. Fortunately, very similar information may be obtained from the C−C skeletal stretching region of the Raman spectra. The band at 1130 cm^{-1} in the Raman spectrum is associated with the in-phase C−C stretching mode of an all-trans segment of the hydrocarbon chain and is known to undergo a reduction in intensity upon introduction of gauche bonds.[51−53] This band is assigned to a C−C skeletal stretching mode in which successive carbon atoms move in opposite directions (a transverse optic mode with wave vector zero). The intensity of this band cannot, however, be attributed solely to chains having an all-trans conformation, as in the case of progression bands in the infrared, as the intensity is found to be nonvanishing even in the liquid state, e.g., of the *n*-alkanes. However, as shown by Pink et al.,[52] and experimentally verified by Snyder et. al,[53] the intensity of the 1130 cm^{-1} band is heavily weighted by conformers having extended all-trans segments. In this model,[52] coupling of the C−C stretching vibration of two trans segments separated by a gauche bond is taken into account. The gauche bond causes the trans segments to vibrate out of phase, and consequently, the intensity decrease per gauche bond is amplified even at low gauche concentrations. Thus, the contribution of conformers having a single gauche bond at the end of the chain to the intensity of the 1130 cm^{-1} band is half that of an all-trans chain, whereas the presence of a single gauche bond at any other position decreases the contribution of such conformers to less than 20%.[52]

The Raman spectra in the C−C skeletal stretching region for intercalated bilayer phase with different concentrations of adsolubilized phenol are shown in Figure 9a. The spectra are normalized with respect to the 760 cm^{-1} C−N$^+$ stretching band. The 760 cm^{-1} band is known to be insensitive to changes in the alkyl chain conformation and has been used as an internal standard in comparing the intensity of the 1130 cm^{-1} band between different systems.[51,52] It may be seen that the intensity of the 1130 cm^{-1} band decreases with increasing concentration of phenol. The normalized intensity of the 1130 cm^{-1} band as a function of the concentration of adsolubilized phenol is shown in Figure 9b. Solubilization of phenol causes a sharp decrease in the intensity of this band up to a phenol/CTA concentration of ∼0.5. Above this concentration, the intensity is essentially constant with a value 0.15 similar to that in liquid *n*-alkanes.

These results along with progression band intensities in the infrared indicate that the two phases of the phenol adsolubilized intercalated surfactant bilayer may be distinguished by the presence or absence of intercalated methylene chains having long-range conformational order or planar all-trans registry. For compositions with a phenol/CTA ratio less than 0.5, there is a steady decrease in the fraction of planar all-trans intercalated chains with increasing phenol concentration. At an adsolubilized-phenol/CTA ratio of ∼0.5, which corresponds to the formation of the phase with the increased lattice spacing of 36.0 Å, planar all-trans chains are completely absent in the intercalated bilayer.

The variation of the intensity of the normalized Raman 1130 cm^{-1} band (Figure 9) is quite different from that of the variation of the intensity of ^{13}C NMR resonance, $I_{35.5}/I_{33.0}$ (Figure 7b). Although the former remains essentially unchanged above a phenol/CTA ratio of 0.5, the NMR intensity ratio shows a sharp increase. Both techniques are sensitive to conformational order in the methylene chain. The ^{13}C NMR intensity $I_{35.5}/I_{33.0}$ is, however, specific to the presence of gauche conformers in the middle of the chain, whereas the Raman 1130 cm^{-1} band intensity, like IR progression band intensity, is specific to long-range trans conformational registry. The concentration of planar methylene chains in the bilayer is drastically reduced in the presence of phenol and no longer exists at a phenol/CTA ratio greater than 0.5. Consequently, the Raman 1130 cm^{-1} band

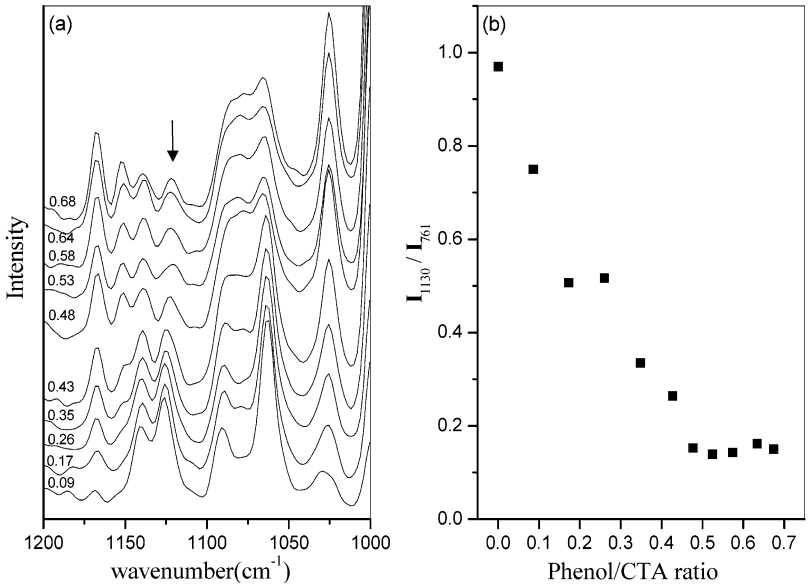

Figure 9. (a) FT-Raman spectra in the skeletal C−C stretching modes region of phenol-adsolubilized−intercalated-bilayer phases, $Cd_{0.83}PS_3(CTA)_{0.34}(phenol)_y$, for different phenol/CTA ratios. (b) The variation of the intensity ratio, I_{1130}/I_{761}, for different phenol/CTA ratios.

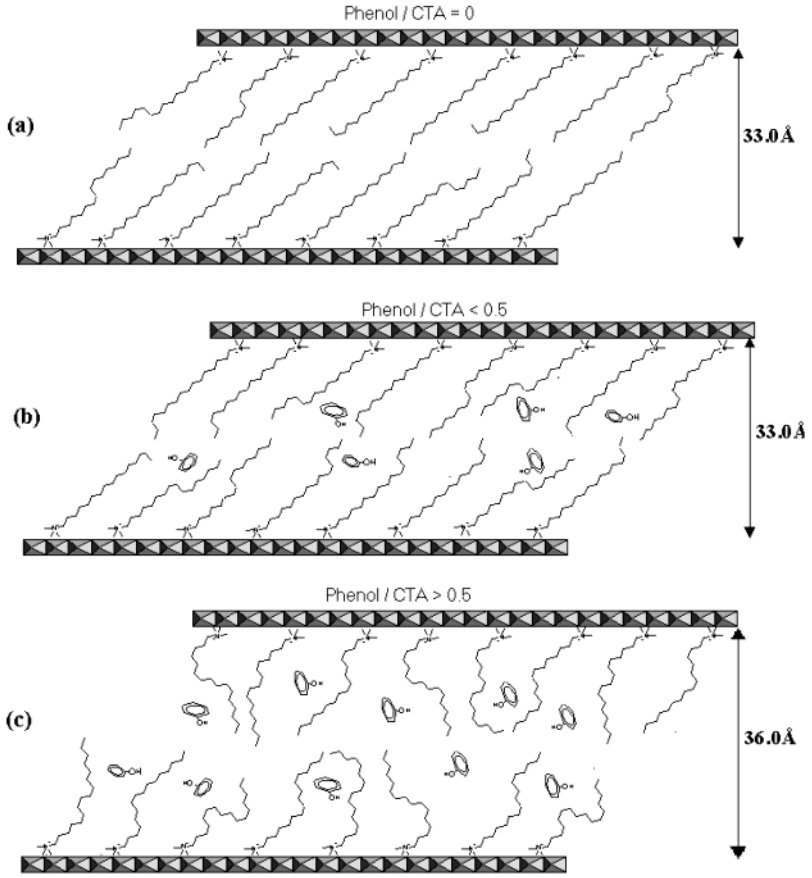

Figure 10. Schematic representation of the effect of adsolubilization of phenol on the conformation of alkyl chain in the intercalated surfactant bilayer, $Cd_{0.83}PS_3(CTA)_{0.34}$. The cation vacancies in the layers are not shown.

intensity shows no change above this ratio. At low phenol concentrations, conformational order is probably destroyed by the generation of gauche defect at the end of the CTA chain.

Conclusions

Phenol molecules have been solubilized in the intercalated surfactant bilayer, $Cd_{0.83}PS_3(CTA)_{0.34}$, formed within the galleries of layered $CdPS_3$ by ion-exchange intercalation of CTA cations. The interaction between the guest phenol and the methylene chains of the host bilayer, which may be regarded as a two-dimensional solvent, are purely dispersive in character, the intercalated CTA ion being devoid of any functional group. Adsorption of phenol from the hexane solution into the bilayer has been studied. The adsorption isotherm and partition coefficient show two regimes depending on the ratio of the concentrations of adsolubilized phenol to intercalated CTA

(phenol/CTA). The two regimes or phases are distinguished by their lattice spacings. For phenol/CTA ratios less than 0.5, the lattice spacing is identical to that of the pure bilayer $Cd_{0.83}PS_3(CTA)_{0.34}$, 33.0 Å, but above this ratio, the lattice spacing shows a further increase of 3.0 Å. The absence of any orientation dependence of the phenolic vibrational modes in the IR spectrum of crystals of $Cd_{0.83}PS_3(CTA)_{0.34}(phenol)_y$ indicate that in both the phases the adsolubilized phenol molecules have no preferred orientation with respect to the interlayer normal, whereas the absence of resonances of the phenolic carbon in the ^{13}C CP-MAS NMR spectra suggests that in the intercalated bilayer the adsolubilized-phenol molecules are rotationally mobile.

Vibrational and ^{13}C NMR spectroscopic measurements provide a detailed description of the effect of the adsolubilized phenol on the conformation of the methylene chains of the intercalated bilayer. In the host bilayer, $Cd_{0.83}PS_3(CTA)_{0.34}$, the majority of the methylene bonds are in the trans conformation and the chains are tilted at an angle of 55° with respect to the normal, consistent with the bilayer thickness of 26.5 Å. The presence of adsolubilized phenol induces conformational (gauche) disorder in the bilayer. At low phenol concentration (phenol/CTA < 0.5), in the phase which shows no change in the lattice spacing from that of the pure bilayer, the presence of adsolubilized phenol causes a decrease in the concentration of methylene chains that have all-trans conformational registry. ^{13}C NMR indicates that this is a consequence of the creation of conformational defects at the chain ends, as evident from the decrease in the intensity of the terminal methyl(C_{16}) resonance in the NMR spectra with increasing phenol concentration. Although the fraction of planar methylene chains in the intercalated bilayer decreases, the lattice spacing shows no change from that of the pure bilayer. At a phenol/CTA ratio of 0.5 or greater, chains with all-trans registry no longer exist in the bilayer, and at this concentration, the lattice spacing increases by 3.0 Å and remains at this value with further increase in phenol concentration. ^{13}C CP-MAS NMR measurements indicate that above a phenol/CTA ratio of 0.5, coinciding with the increased lattice spacing, there is a sharp increase in conformational disorder in the interior or middle of the methylene chains of the intercalated bilayer.

These observations allows for a rationalization of the changes in the lattice spacing with concentration of adsolubilized phenol. For a solute molecule like phenol to be accommodated within the intercalated bilayer, void space should be available.[16] In the host bilayer, $Cd_{0.83}PS_3(CTA)_{0.34}$, the average distance between methylene chains is 9.2 Å[22] (in comparison, the cross-sectional diameter of an all-trans methylene chain is 5.2 Å). The bilayer can therefore accommodate phenol molecules at low concentrations with no change in lattice spacing. Below a phenol/CTA ratio of 0.5, although there is a decrease in the concentration of all-trans methylene chains, there is still a finite concentration of planar all-trans chain in the bilayer. These chains maintain the same tilt angle as in the pure bilayer, and consequently, the lattice spacing remains unchanged. It may be noted that even for the pure bilayer only a fraction of the total concentration of the intercalated surfactant chains are in an all-trans planar conformation at 300 K.[45,46] For phenol molecules to be accommodated above a phenol/CTA ratio of 0.5, additional void space needs to be created; this requires generation of conformational defects in the interior (C_4-C_{13}) of the methylene chains. In an ordered arrangement in which all grafted methylene chains are essentially planar and have identical tilt angles, it is not possible to create gauche defects in the interior of the methylene chains because of the extra volume required for such conformers (for a grafted surfactant chain lateral expansion is not possible). Space for the creation of such conformers can be created only if the chains are "pushed away" from each other by acquiring different tilt angles. The loss of "tilt coherence" leads to the observed lattice expansion. This is illustrated schematically as a cartoon in Figure 10. The value of the phenol/CTA ratio of 0.5, which separates the two phases, is probably significant because at this concentration every CTA chain in the bilayer would be in contact with at least one phenol molecule (assuming uniform distribution).

The results presented here have allowed us to relate changes in the conformation of the methylene chain of the intercalated bilayer on adsolubilization of phenol, as measured by vibrational and ^{13}C NMR spectroscopy, with changes in the interlamellar spacing as determined by X-ray diffraction. The present work has also demonstrated how the host−guest chemistry of layered $CdPS_3$ can be extended to include guest molecules such as phenol. As mentioned in the Introduction, $CdPS_3$ and other members of the divalent metal thiophosphate family exhibit an unique ion-exchange intercalation reaction, in which guest species from aqueous solution are introduced into the interlamellar region with an equivalent loss of metal ions from the layers.[19−21,54] The host−guest chemistry is, however, restricted to further exchange of the interlamellar ions by other cations[55,56] and to a limited extent, adsorption of polar molecules, e.g., poly(ethylene oxide)[57,58] and crown ethers,[59] through ion−dipole interactions. We have shown that by functionalizing the internal surface of $CdPS_3$ by forming an intercalated surfactant bilayer guest molecules such as phenol can now be inserted, which was hitherto not possible.

Supporting Information Available: Table giving the positions of the infrared and Raman bands, and their assignments, for the intercalated bilayer, $Cd_{0.93}PS_3$ $(CTA)_{0.34}$, and the phenol solubilized intercalated bilayer, $Cd_{0.93}PS_3$ $(CTA)_{0.34}$ $(phenol)_y$. This material is available free of charge via the Internet at http://pubs.acs.org.

References and Notes

(1) Wolfe, T. A.; Demirel, T.; Baumann, R. *Clays Clay Miner.* **1985**, *33*, 301.
(2) Mortland, M. M.; Shaobai, S.; Boyd, S. A. *Clays Clay Miner.* **1986**, *34*, 581.
(3) Holsen, T. M.; Taylor, E. R.; Seo, Y. C.; Anderson, P. R. *Environ. Sci. Technol.* **1991**, *25*, 1585.
(4) Brown, M. J.; Burris, D. R. *Groundwater* **1996**, *34*, 734.
(5) LeBaron, P. C.; Wang, Z, Pinnavia, T. J. *Appl. Clay Sci.* **1999**, *15*, 11.
(6) Giannelis, E. P.; Krishnamoorti, R.; Manias, E. *Adv. Polym. Sci.* **1999**, *138*, 107.
(7) Alexandre, M.; Dubois, P. *Mater. Sci. Eng.* **2000**, *28*, 1.
(8) Ogawa, M.; Kuroda, K. *Bull. Chem. Soc. Jpn.* **1997**, *70*, 2593.
(9) Williams, S.; Becerro, A. I.; Castro, M. A.; Thomas, R. K. *Physica B* **1997**, *234−236*, 1096.
(10) Esumi, K.; Takeda, Y.; Goino, M.; Ishiduki, K.; Koide, Y. *Langmuir* **1997**, *13*, 2585.
(11) Becerro, A. I.; Castro, M. A.; Thomas, R. K. *Colloids Surf. A* **1996**, *119*, 189.
(12) Robins, D. S.; Dutta, P. K. *Langmuir* **1994**, *12*, 402.
(13) Matsuo, Y.; Hatase, K.; Sugie, Y. *Chem. Commun.* **1999**, *1*, 43.
(14) Weiss, A. *Angew. Chem., Int. Ed. Engl.* **1963**, *2*, 134.
(15) Jordon, J. M. *J. Phys. Colloid. Chem.* **1950**, *54*, 294.
(16) Dorsey, J. G.; Dill, K. A. *Chem. Rev.* **1989**, *89*, 331.
(17) Ouvrard, G.; Brec, R.; Rouxel, J. *Mater. Res. Bull.* **1985**, *20*, 1181.
(18) Brec, R. *Solid State Ionics* **1986**, *22*, 3.
(19) Clement, R. *J. Chem. Soc., Chem. Commun.* **1980**, 647.
(20) (a) Clement, R.; Garnier, O.; Jegoudez, J. *Inorg. Chem.* **1986**, *25*, 1404. (b) Clement, R; Audiere, J. P.; Renard, J. P. *Rev. Chim. Miner.* **1982**, *19*, 560.
(21) Jeevanandam, P; Vasudevan, S. *Solid State Ionics* **1997**, *104*, 45.

(22) Venkataraman, N. V.; Vasudevan, S. *J. Phys. Chem. B* **2001**, *105*, 1805.
(23) Klingen, V. W.; Ott, R.; Hahn, H. *Z. Anorg. Allg. Chem.* **1973**, *396*, 271.
(24) Arun, N.; Vasudevan, S.; Ramanathan, K. V. *J. Am. Chem. Soc.* **2000**, *122*, 6028.
(25) Venkataraman, N. V.; Vasudevan, S. *J. Phys. Chem. B* **2000**, *104*, 11179.
(26) Hoiland, H.; Blokhus, A. M. In *Handbook of Applied Surface and Colloid Chemistry*; Birdi, K. S., Ed.; CRC Press: New York, 1997.
(27) Snyder, R. G. *J. Mol. Spectrosc.* **1964**, *7*, 116.
(28) Snyder, R. G. *J. Chem. Phys.* **1979**, *71*, 3229.
(29) Varsanyi, G. *Vibrational Spectra of Benzene Derivatives*; Academic Press: New York, 1969.
(30) Roth, W.; Imhof, P.; Gerhards, M.; Schumm, S.; Kleinermanns, K. *Chem. Phys.* **2000**, *252*, 247.
(31) Soderlind, E.; Stilbs, P. *Langmuir* **1993**, *9*, 1678.
(32) Khimyak, Y. Z.; Klinowski, J. *Phys. Chem. Chem. Phys.* **2001**, *3*, 616.
(33) Zerbi, G. In *Modern Polymer Spectroscopy*; Zerbi, G., Ed; Wiley-VCH: New York, 1999.
(34) Snyder, R. G. *J. Chem. Phys.* **1967**, *47*, 1316.
(35) MacPhail, R. A.; Strauss, H. L.; Snyder, R. G.; Elliger, C. A. *J. Phys. Chem.* **1984**, *88*, 334.
(36) Snyder, R. G.; Strauss, H. L.; Elliger, C. A. *J. Phys. Chem.* **1982**, *86*, 5145.
(37) Wallach, D. F. H.; Verma, S. P.; Fookson, J. *Biochim. Biophys. Acta* **1979** *559*, 153.
(38) Snyder, R. G.; Scherer, J. R. *J. Chem. Phys.* **1979**, *71*, 3221.
(39) Snyder, R. G.; Scherer, J. R.; Gaber, B. P. *Biochim. Biophys. Acta* **1980**, *601*, 47.
(40) Chachaty, C. *Prog. Nucl. Magn. Reson. Spectrosc.* **1987**, *19*, 183.
(41) Lindman, B.; Soderman, O.; Stilbs, P. In *Surfactants in Solution*; Mittal, K. L, Ed.; Plenum Press: New York, 1989; Vol. 7, p 1.
(42) Wang, L.-Q.; Liu, J.; Exarhos, G. J.; Flanigan, K. Y.; Bordia, R. *J. Phys. Chem. B* **2000**, *104*, 2810.
(43) Kolodziejski, W.; Klinowski, J. *Chem. Rev.* **2002**, *102*, 613.
(44) Venkataraman, N. V.; Vasudevan, S. *J. Phys. Chem. B* **2001**, *105*, 7639.
(45) Spiess, H. W. In *Encyclopedia of Nuclear Magnetic Resonance*; Grant, D. M., Harris, R. K., Eds; John Wiley & Sons: New York, 1996; Vol. 6, p 3668.
(46) Venkataraman, N. V.; Vasudevan, S. *Proc. Indian Acad. Sci.*, (*Chem. Sci.*) **2001**, *113*, 539.
(47) Snyder, R. G. *J. Mol. Spectrosc.* **1960**, *4*, 411.
(48) Snyder, R. G.; Schachtschnelder, J. H. *Spectrochim. Acta* **1963**, *19*, 85.
(49) Tasumi, M.; Shimonauchi, T.; Miyazwa, Y. *J. Mol. Spectrosc.* **1962**, *9*, 261
(50) Venkataraman, N. V.; Vasudevan, S. *J. Phys. Chem. B* **2002**, *106*, 7766.
(51) Gaber, B. P.; Peticolas, W. L. *Biochim. Biophys. Acta* **1977**, *465*, 260.
(52) Pink, D. A.; Green, T. J.; Chapmann, D. *Biochemistry* **1980**, *19*, 349.
(53) Snyder, R. G.; Cameron, D. G.; Casal, H. L.; Compton, D. A. C.; Mantsch, H. H. *Biochim. Biophys. Acta* **1982**, *684*, 111.
(54) Joy, P. A.; Vasudevan, S. *J. Am. Chem. Soc.* **1992**, *114*, 7792.
(55) Lacroix, P.; Audiere, J. P.; Clement, R. *J. Chem. Soc., Chem. Commun.* **1989**, 536.
(56) Field, C. N.; Boillot, M. L.; Clement, R. *J. Mater. Chem.* **1998**, *8*, 283.
(57) Lagadic, I.; Leaustic, A.; Clement, R. *J. Chem. Soc., Chem. Commun.* **1992**, 1396.
(58) Jeevanandam, P.; Vasudevan, S. *Chem. Mater.* **1998**, *10*, 1276.
(59) Glueck, D. S.; Brough, A. R.; Mountford, P.; Green, M. L. H. *Inorg. Chem.* **1993**, *32*, 1893.